

Solar cycle variations in the ionosphere of Mars

Beatriz SÁNCHEZ-CANO¹, Mark LESTER¹, Olivier WITASSE²,
Pierre-Louis BLELLY³, Marco CARTACCI⁴, Sandro M. RADICELLA⁵,
Miguel HERRAIZ^{6,7}

¹ Radio and Space Plasma Physics Group, Physics and Astronomy Department, University of Leicester, Leicester, United Kingdom, bscmdr1@leicester.ac.uk, ² European Space Agency, ESTEC – Scientific Support Office, Noordwijk, The Netherlands. ³ Institut de Recherche en Astrophysique et Planétologie, Toulouse, France. ⁴ Istituto di Astrofisica e Planetologia Spaziali (IAPS), Istituto Nazionale di Astrofisica (INAF), Rome, Italy. ⁵ Abdus Salam International Centre for Theoretical Physics (ICTP), Telecommunications / ICT for Development Laboratory, Strada Costiera 11 I-34151, Trieste, Italy. ⁶ Departamento de Física de la Tierra, Astronomía y Astrofísica I, Universidad Complutense de Madrid, Spain. ⁷ Instituto de Geociencias, (UCM, CSIC), Madrid, Spain.

Recibido: 01/04/2016

Aceptado: 06/08/2016

Abstract

Solar cycle variations in solar radiation create notable changes in the Martian ionosphere, which have been analysed with Mars Express plasma datasets in this paper. In general, lower densities and temperatures of the ionosphere are found during the low solar activity phase, while higher densities and temperatures are found during the high solar activity phase. In this paper, we assess the degree of influence of the long term solar flux variations in the ionosphere of Mars.

Key words: solar cycle; ionosphere of Mars; TEC.

Variaciones de la ionosfera de Marte debidas al ciclo solar

Resumen

La radiación solar en cada fase del ciclo solar crea importantes variaciones en la ionosfera de Marte, las cuales son analizadas en este artículo con datos de la sonda Mars Express. En general, las densidades y temperaturas más bajas de la ionosfera se encuentran durante la fase de baja actividad solar, mientras que las densidades y temperaturas más elevadas se encuentran durante la fase de alta actividad solar. Este artículo evalúa el efecto que las variaciones del flujo solar tienen a largo plazo en la ionosfera.

Palabras clave: ciclo solar; ionosfera de Marte; TEC.

Summary: Introduction 1. Mars Express dataset 2. Ionospheric behaviour with the solar cycle 3. Discussion: Earth ionosphere comparison. 4. Conclusions. Acknowledgments. References.

Normalized Reference

Sánchez-Cano, B., Lester, M., Witasse, O., Blelly, P-L., Cartacci, M., Radicella, S.M., Herraiz, M., (2016). Solar cycle variations in the ionosphere of Mars, *Física de la Tierra*, Vol., 28, 97-110.

Introduction

The ionosphere is the conductive atmospheric layer formed by the ionization of the neutral atmosphere. This layer contains a significant number of free thermal electrons and ions, which are commonly produced via ionization of the neutral particles by extreme ultraviolet/X-ray radiation from the Sun and by collisions with energetic particles that penetrate the atmosphere (e.g. Schunk and Nagy, 2009).

In the particular case of Mars, solar extreme-ultraviolet (EUV) photons between 10 nm and 90 nm are responsible for the creation of the main layer of its ionosphere (e.g. Witasse et al., 2008). The maximum density of this layer is typically located between 125-140 km altitude with a characteristic electron density range between $0.4 \cdot 10^{11}$ and $2 \cdot 10^{11}$ electrons per m^{-3} , and is dependent on solar zenith angle (SZA) and solar activity conditions (e.g. Gurnett et al., 2005; Witasse et al., 2008; Peter et al., 2014; Sánchez-Cano, 2014). Since EUV photons are greatly attenuated at lower atmospheric altitudes, soft X-ray solar photons of 10 nm are the dominant flux able to ionize the lower atmosphere, with a significant contribution due to secondary electrons and photoelectrons. This secondary layer is typically located at around 110-115 km altitude (e.g. Schunk and Nagy, 2009; Sánchez-Cano, 2014), and is considerably weaker than the main peak but it is not negligible since it contributes to about 10% of the Total Electron Content (Sánchez-Cano et al., 2015a). Photochemical processes control the behaviour of the two main ionospheric layers at Mars up to 170-200 km altitude (e.g. Schunk and Nagy, 2009), and in this regime, the Martian ionosphere is well represented, at least to first order, by an α -Chapman-type layer (e.g. Gurnett et al., 2005; Withers, 2009; Němec et al., 2011; Sánchez – Cano et al., 2013; 2014).

Ionospheric variability can be caused by many factors. External factors such as the solar cycle, solar flares, coronal mass ejections (CMEs) or Corotating Interaction Regions (CIR), among others contribute significantly. In addition, the planet's relatively elliptical orbit around the Sun is a factor of major impact, as the seasons, distance to the Sun and the diurnal variation have a major role in determining ionospheric structure. Moreover, the planet is also a major source of variability in the ionosphere, as dust storms, thermal atmospheric tides, crustal magnetic fields, or the topography itself modulate the behaviour of the ionosphere (e.g. Shinagawa and Cravens, 1989; Witasse, 2000; Withers et al., 2003; Morel et al., 2004; Wang and Nielsen, 2004; Mendillo et al., 2006; Němec et al., 2011; Zou et al., 2011; Withers et al., 2012a, b; González-Galindo et al., 2013; Withers and Pratt, 2013; Bougher et al., 2015; Matta et al., 2015; Sánchez-Cano et al., 2015b, 2016). However, the solar cycle is the factor that plays the most important long-term role in ionospheric variability, as each solar cycle phase produces changes in the neutral atmosphere, in the ionospheric temperatures and in the densities. A good knowledge of the solar cycle variations in the ionosphere of Mars is therefore essential to fully understand the long-term Martian ionospheric variability, its interaction with the solar wind and facilitate satellite communications at Mars.

In this paper, we focus on the variability created by external factors due to long-term variations in the solar EUV and X-ray fluxes, i.e. solar cycle phases at Mars. The behaviour of the ionosphere of Mars in response to the long-term variability produced by the solar cycle evolution is assessed from a number of different ionospheric parameters.

1. Mars Express dataset

Since the Sun is the main source of ionization in the Martian upper atmosphere, the ionospheric behaviour as a function of solar cycle is directly dependent on its radiation behaviour with time. Only now, thanks to the more than 10 years of data from Mars Express (Chicarro et al., 2004), is it possible to analyse the ionospheric response to changes in the solar activity during a full solar cycle with the same dataset and with an almost complete planetary coverage.

The main dataset used in this study is the Mars Advanced Radar for Subsurface and Ionospheric Sounding (MARSIS) (Picardi et al., 2004) on board the Mars Express (MEX) spacecraft (Chicarro et al., 2004). This instrument has been probing the ionosphere and subsurface of Mars since mid-June 2005 (Orosei et al., 2014). MARSIS has two different operational modes, from which multiple ionospheric parameters can be obtained. When working in the Active Ionospheric Sounding (AIS) mode (Gurnett et al., 2005; Orosei et al., 2014), MARSIS works as a topside ionospheric sounder, where the ionization from the spacecraft to the maximum ionization region (~135 km for pure dayside conditions) is sampled. The vertical electron density profiles of the topside ionosphere are the main data product (Sánchez – Cano et al., 2012; Morgan et al., 2013).

When MARSIS works in the subsurface mode (Gurnett et al., 2005; Orosei et al., 2014), the instrument works as a geophysical radar to analyse the subsurface of the planet. The total electron content (TEC) of the entire ionosphere (from Mars' surface to spacecraft position) can be retrieved as a by-product (Cartacci et al., 2013) because the radar signals twice cross the full ionosphere (from MEX to the surface and then back to MEX) and the plasma slows the signal propagation, from which, TEC is retrieved. Subsurface TEC data have, however, daylight limitations as they are less trustable in the full dayside when the MARSIS carrier frequencies are close to the maximum plasma frequency of the ionosphere. In these cases, a signal degradation is manifest (Sánchez-Cano et al., 2015a). In this study, subsurface TEC is analysed through the Cartacci et al. (2013) algorithm, only with data that fit the Signal-to-Noise Ratio (SNR) condition of $\text{SNR} > 25$ dB. This conservative approach guarantees the accuracy of the TEC estimation (Sánchez-Cano et al., 2016).

2. Ionospheric behaviour with the solar cycle

Solar cycle variations in solar radiation create notable changes in the Martian ionosphere. For the same level of solar activity, the ionosphere of Mars behaves notably different depending on each phase of the solar cycle (see Figure 2 of Sánchez-Cano et al., 2015b). To illustrate the general behaviour in density of the ionosphere of Mars with the solar cycle, a case study is presented in Figure 1. This figure shows 41 MARSIS AIS electron density profiles from four representative Mars Express orbits across four panels. Each panel represents a different phase of the latest solar cycle, i.e. moderate declining phase, low solar activity phase, moderate ascending phase and high solar activity phase, while all the profiles have the same illumination characteristics, i.e. the solar zenith angle is between 45 and 55 degrees. In order to avoid a possible magnetic field influence, the profiles were selected over regions without the presence of crustal magnetic anomalies as indicated by the Cain et al. (2003) magnetic field model (<3 nT at the spacecraft position). In each panel, two Chapman layers have been plotted as a reference to evaluate the degree of variation of the AIS profiles: the dashed line assumes a constant scale height with altitude, while the solid line considers a scale height that increases linearly with altitude, as modelled by Sánchez-Cano et al. (2013). Both lines stop at 200 km in accordance with the average limit of the photochemical region. Nevertheless, both lines have been extrapolated to higher altitudes (dash-point lines) in order to estimate a possible profile behaviour if the photochemical regime were valid at those altitudes.

Panels A and C represent two orbits from periods of moderate solar activity, with Panel A during the declining phase of the solar cycle and Panel C from the ascending phase. Profiles from an orbit from the very low activity of solar minimum phase is plotted in Panel B and an orbit from close to solar maximum in panel D.

In the moderate activity cases (panels A and C), the shapes of the ionospheric profiles are very similar, despite possible solar radiation differences during the declining and increasing phases of the solar cycle. However, when the solar cycle is at its extremes, the electron density does not follow this trend. Focusing on the period of solar minimum (panel B), a notable difference in density is found. We believe that this is a consequence of a cooler ionosphere and thermosphere, as suggested by Sánchez-Cano et al. (2015b). Also, there is evidence for two density regimes. From the peak to ~ 180 km, the profile is consistent with a Chapman layer with a constant scale height (photochemical region). However, above this, the topside behaviour responds to the diffusive region regime, being better reproduced with a scale height that increases only slowly with altitude if the photochemical laws were still valid in that regime.

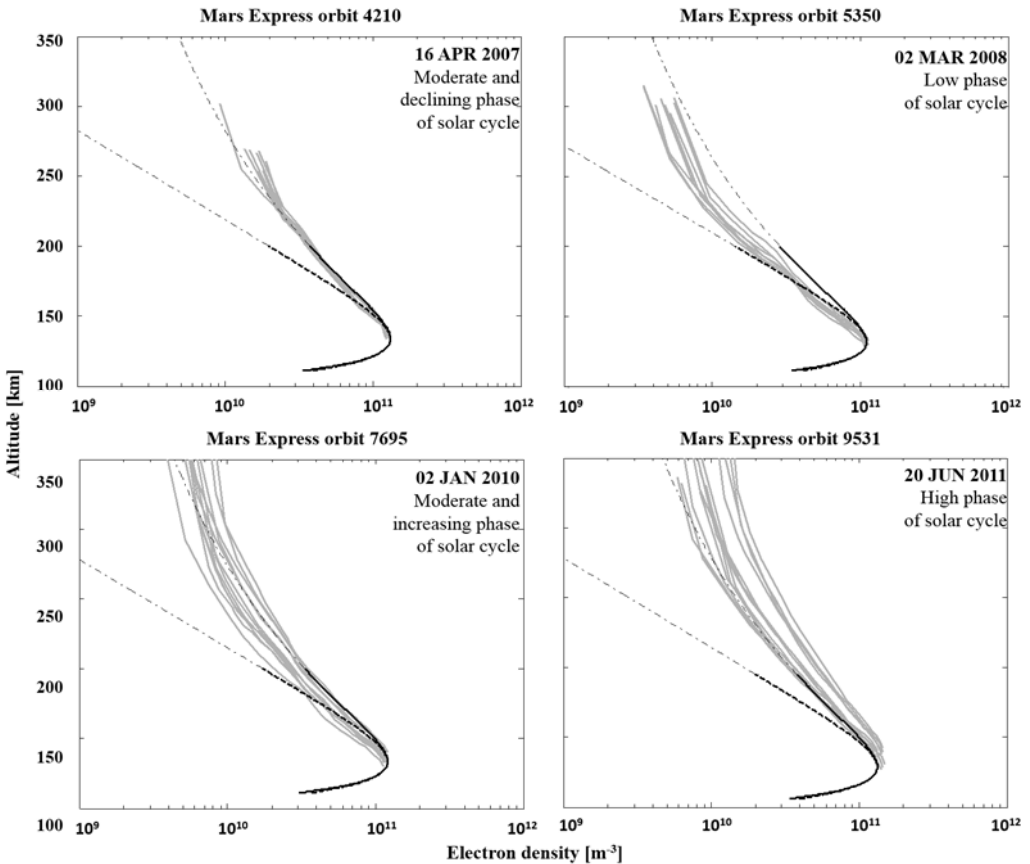


Figure 1. Electron density profiles of four Mars Express orbit examples belonging to different phases of the solar cycle. In all of them, two Chapman layers are plotted as a reference to evaluate the degree of variation of the profiles: a Chapman layer with a constant scale height (dash-line), and a Chapman layer with a linear altitude-variable scale height (solid-line). In the four cases, the solar zenith angle of all the profiles is between 45 and 55 degrees.

Most probably, this second regime is the consequence of an induced magnetic field from solar wind origin (Sánchez-Cano et al., 2015b). This period was characterized by an especially prolonged solar minimum, which was deeper than the previous solar minimum: the EUV radiation was extremely reduced from end 2007 to end 2009 and X-rays were practically absent (Sánchez-Cano et al., 2015b; 2016). In contrast, profiles from the period of high solar activity are shown in panel D. These profiles show a notable increase in density, with respect to the other periods. The altitude of

the peak density is higher than the reference altitude for some cases, thus highlighting that the neutral density of the atmosphere could also have increased.

A more detailed and global analysis is presented in Figure 2, where the evolution of several parameters during 6 terrestrial years is shown. In the first panel, the two most characteristic solar irradiance fluxes able to ionize the ionosphere of Mars have been plotted. The EUV solar flux measured by the Thermosphere, Ionosphere, Mesosphere Energetics and Dynamics (TIMED)-Solar EUV Experiment (SEE) satellite (Woods and Eparvier, 2006) at the wavelength of 30.5 scaled to the Mars heliocentric distance is shown (in black), together with the X-ray background radiation measured by the Geostationary Operational Environmental Satellite (GOES) family of satellites extrapolated also to the Mars location (in grey). Using these parameters, the interval is divided into 4 subintervals, each one with different solar radiation characteristics, following exactly the same criteria as Sánchez-Cano et al. (2015b, 2016). Period A corresponds to the moderate solar activity phase of the solar cycle in the declining phase of the solar cycle 23, from 2006 to mid-2007. This period was characterised by moderate values of both EUV and X-ray fluxes. Period B corresponds to the low solar activity phase of the solar cycle 23/24, from mid-2007 to mid-2009. This period was characterized by a lower general reduction of EUV in comparison to the former period, and a notable reduction (near permanent absence) of measurable X-ray flux. Period C corresponds to the moderate solar activity in the ascending phase of the solar cycle 24, from mid-2009 to mid-2011. During this phase, every flux parameter showed similar levels to those in Period A, with a progressive ascending trend along the period. Finally, Period D corresponds to the high activity phase of the solar cycle 24, from mid-2011 to 2012. On average, both radiation fluxes were higher in Period D than in the other three periods.

In the second panel, the daily average TEC of the full atmosphere of Mars for a narrow interval of SZA between 68 and 73 degrees (grey dots) has been plotted, together with the difference of pressures (in black) between the maximum plasma pressure (at the main peak of the ionosphere) and the solar wind pressure at Mars. These two pressures are also individually plotted in the third panel. The maximum thermal pressure at Mars has been calculated from the plasma scale height of the MARSIS AIS profiles as in Sánchez-Cano et al. (2016), and the solar wind pressure at Mars come from the Advanced Composition Explorer (ACE) satellite and from the Operating Missions as a Node on the Internet (OMNI) solar wind databases at 1 AU extrapolated to Mars' distance. In the fourth panel, the daily neutral (in grey) and plasma (in black) average temperatures at the altitude of the main ionospheric peak have been plotted. These parameters were obtained from the daily average scale height (neutral and plasma respectively) of the MARSIS AIS electron density profiles as described in detail in Sánchez-Cano et al. (2016). In this latest work, one neutral scale height that depends on solar zenith angle and on altitude above the main peak is obtained for each phase of the solar cycle (same phases than in this work). Therefore,

a single neutral temperature value that depends on solar zenith angle and altitude is obtained for each phase of the solar cycle after considering equation (1).

$$H = k_B T / mg \quad (1)$$

$$H = - dh / d(\ln N) \quad (2)$$

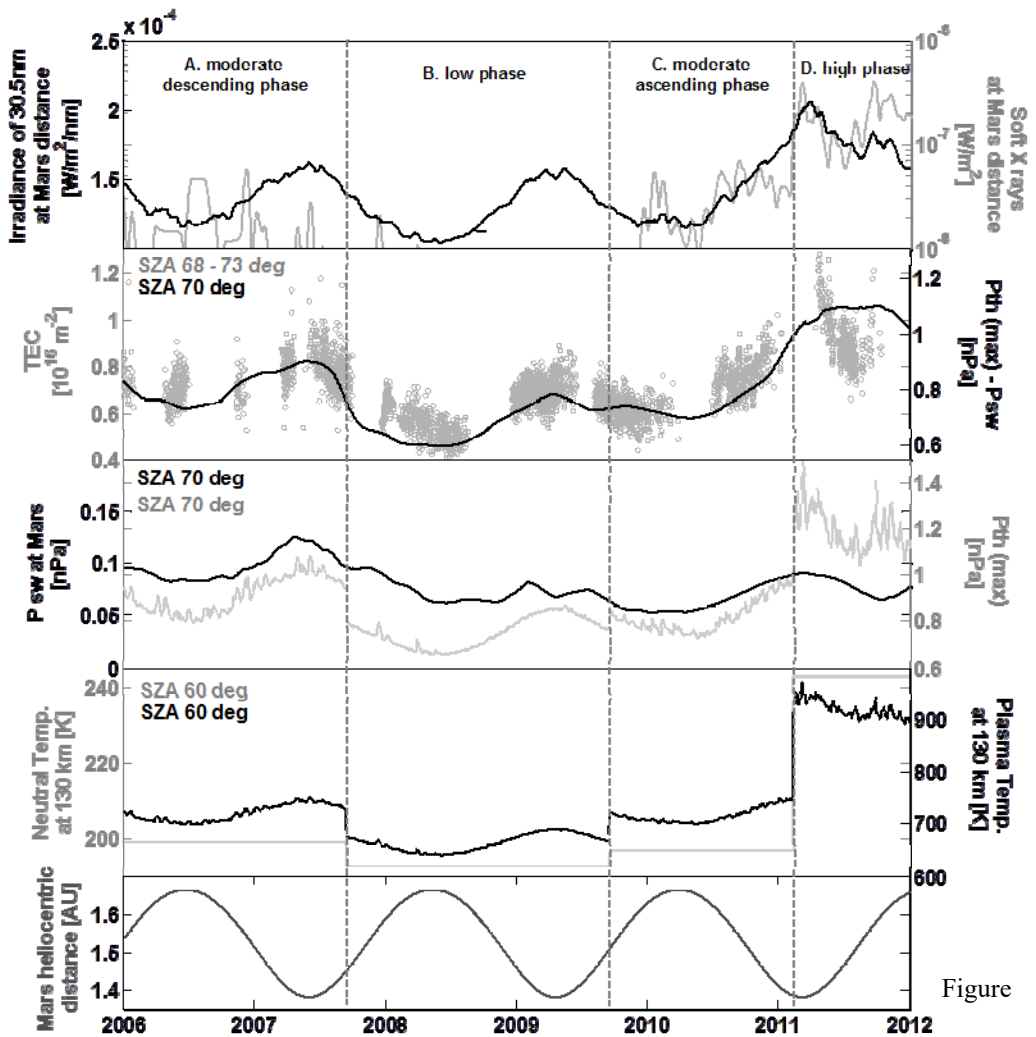
where H is the scale height, m is the mean molecular mass of the medium, T is its temperature, g is the acceleration due to the gravity of the planet at ionospheric altitudes, k_B is the Boltzmann constant, h is the height and N the electron density.

The plasma temperature was obtained with equation (2) after considering the NeMars empirical model (Sanchez-Cano et al., 2013) to reconstruct the electron density profile and each of the previous neutral scale heights of each solar cycle phase. The best linear fit to the region of the reconstructed electron density profile close to the main peak (equation 2), and considering equation (1), gives the average plasma temperature at the peak of the ionosphere. Since the NeMars model varies with solar activity, as a function of the F10.7 index, and with heliocentric distance, the average plasma temperature also varies with them. Therefore, both temperatures should be treated as the average temperature of each solar phase and the steps between periods are an artefact of dividing the interval into four subintervals.

Finally, in the fifth panel, the Mars' heliocentric distance has been plotted to help in the discussion.

The Martian ionospheric behaviour is expected to follow the solar flux pattern, since it is directly dependent on the incident EUV and X-ray radiation. As observed in the second and fourth panels, TEC and temperatures have a similar trend to that of the EUV flux at Mars, with a modulation in magnitude related to the X-ray flux intensity. The daily TEC as well as EUV flux, are strongly influenced by the heliocentric distance of Mars. This is illustrated by the sinusoidal-shape of the curve, where TEC is larger when Mars is closer to the Sun, and lesser when is at the furthest place.

According to the solar cycle phases, TEC is clearly reduced during the period of low solar activity due to a large reduction of the EUV flux and to the absence of X-ray measurable flux. This produced a decrease in TEC to $7 \times 10^{15} \text{ m}^{-2}$ during the 2008-2009, compared to $8 \times 10^{15} \text{ m}^{-2}$ in 2006-2007 and 2010-2011 (moderate solar activity descending and ascending phases respectively). At solar maximum, starting at late 2011, TEC increased because of a much larger EUV and X-ray fluxes, with values of order $10 \times 10^{15} \text{ m}^{-2}$. Note that these values vary along the elliptic orbit of Mars around the Sun and so the values have been taken at about the same phase in the orbit, showing a clear TEC season dependence on the solar cycle. The daily evolution of the TEC of the full atmosphere follows very closely the behaviour of the pressure difference plot, suggesting that the Martian plasma system is consistently driven by the relationship between the solar wind dynamic pressure and the maximum thermal pressure of the ionosphere (Sánchez-Cano et al., 2016).



Figure

Figure 2. First panel: EUV solar irradiance at the wavelength of 30.5 nm at Mars distance (black, left axis). Solar X-rays at Mars distance (grey, right axis). Second panel: TEC of the full ionosphere from MARSIS in the subsurface mode (grey, left axis). Pressure difference between the maximum thermal pressure and the solar wind pressure (black, right axis). Third panel: Solar wind pressure at Mars location (black, left axis). Maximum thermal pressure (at the main peak of the ionosphere, grey, right axis). Fourth panel: neutral (grey, left axis) and plasma (electron and ions) (black, right axis) temperatures at the peak ionospheric region. Fifth panel: Mars heliocentric distance. Vertical lines designate the solar cycle phases. Note that the steps between periods in panels 3 and 4 are an artefact of dividing the interval into four subintervals as explained in the text.

A similar behaviour is observed with both temperatures, as both curves also follow the solar cycle radiation pattern. For a SZA of 60 degrees, the neutral temperature at both periods of moderate solar activity is ~ 200 K, while the plasma temperature is ~ 700 K. However, both temperatures suffered a general reduction during the period of low solar activity, where the neutral temperature was ~ 20 K cooler and the plasma ~ 50 K cooler. On the other hand, higher neutral and plasma temperatures are found in the high solar activity period, where an increment of 40 K and 200 K respectively was found.

Therefore, solar cycle variations can be identified in the ionosphere of Mars in the form of changes in density, TEC, pressure balance and average plasma temperature. EUV flux is the major driver of these variations together with the soft X-ray radiation, which both together create unique characteristics in the behaviour of the martian ionosphere with each phase of the solar cycle. These results agree with the findings of Sánchez-Cano et al., 2015b, where it was demonstrated that for same levels of solar activity, the ionosphere of Mars behaves different at each phase of the solar cycle. Moreover, solar cycle variations can lead to significant changes in the atmospheric escape rate, as EUV intensity and solar wind velocity play a major role on it (Ramstad et al., 2015).

3. Discussion: Earth ionosphere comparison

We have shown that the long-term variability is an important factor to consider for the evolution of the Martian ionosphere. Moreover, the heliocentric distance plays an important role modulating the intensity of the incoming solar radiation, and therefore, the temperature, TEC, density and pressure balance of the upper atmosphere at Mars.

If this ionospheric response is compared with the well-known Earth ionosphere behaviour, a number of similarities can be found despite Mars not having a global-inner magnetic field, as well as different atmospheric composition and size, and an orbit which is further away from the Sun. Both ionospheres strictly depend on the EUV variation at their orbits and are modulated by the X-ray flux (e.g. Kutiev et al. 2013 for the Earth case). At Earth, the solar cycle drives large temperature differences in the thermosphere, which causes an even larger density change in the upper atmosphere (e.g. Solomon et al. 2011). However, the terrestrial ionosphere shows a weak dependence on the heliocentric distance because the Earth orbit around the Sun can be considered quasi-circular, especially when compared to the high elliptically Mars' orbit. Therefore, the main difference is that the EUV spectrum at Earth does not exhibit any sinusoidal shape as in the case of Mars (first panel Figure 2).

Nevertheless, the vertical structure of both Earth's and Mars' dayside ionospheres respond analogously to the solar cycle variability. Both ionospheres have largest TEC values during solar maximum, being therefore warmer and with a larger inner thermal pressure. Moderate solar activity periods have characteristics halfway between high

and low solar activity phases, while at solar minimum the lower TEC values, temperatures and inner thermal pressure are found. An important mention should be made to the latest solar minimum (end 2007 to end 2009), when an exceptional low level of solar activity took place. This minimum was lower and longer than previous solar minimum and the modelling of the ionosphere of both planets showed deficiencies in the predictions for local and global conditions (e.g. Klenzing et al., 2013; Yue et al., 2013; Sánchez-Cano et al., 2015b). There is much evidence that indicates that Earth's thermosphere was much colder and lower in density than expected by previous minima (e.g. Solomon et al., 2010, 2011, 2013). This is also confirmed in the case of Mars.

We have shown that during the low solar activity phase, a much lower density in the ionosphere is found. Similarly, the recent work of Withers et al. (2014) showed the intense decrease of the peak density for the low solar activity period (Figure 2 at Withers et al., 2014). Furthermore, in this work we have demonstrated that the photochemical region ended at about 20 km lower than in both moderate solar activity phases (Figure 1), mostly due to a more permanent magnetized state of the ionosphere as stated by Sánchez-Cano et al. (2016). The thermosphere was also cooler, as indicated by the temperatures of the neutrals and plasma constituents at ~135 km in Figure 2, and also a clearly reduced TEC is found only for that period.

This work has only focused on the region of the planet without the presence of crustal magnetic anomalies, which is the major part of the planet (e.g. Cain et al., 2003). However, crustal magnetic fields have an important role at high altitudes. As Němec et al. 2016 have recently demonstrated, electron densities at high altitudes (in the diffusive region) are significantly increased over crustal magnetic field areas, while peak electron densities are nearly unaffected. Moreover, there is clear evidence that solar flux at these high altitudes is still significant (Němec et al., 2016), the evolution of which with the solar cycle constitutes a clear future line of work.

4. Conclusions

To conclude, the solar cycle is an important factor to take into account in the long-term evolution of the Martian ionosphere, as the different solar phases determine the role of the plasma system behaviour. A good modelling of the ionosphere is essential to fully understand the role of the upper atmosphere interaction with the solar wind, the reaction of the ionosphere to short and intense space weather events, such as interplanetary coronal mass ejections or stream interaction regions, among others, or the atmospheric scape over time. Moreover, from the technological point of view, these solar cycle variations affect the satellite communication and navigation, as the ionosphere interferes and distorts the signals and can cause different levels of drag on spacecraft.

Acknowledgments

B.S.-C. and M.L. acknowledge support through STFC grant ST/K001000/1 and ST/N000749/1. B.S.-C. also acknowledges a scientific stay at ESA-ESTEC by ESTEC Faculty support funding. Authors acknowledge Mars Express MARSIS PIs for making data accessible.

5. References

- BOUGHER, S. W., PAWLOWSKI, D., BELL, J.M., NELLI, S., MCDUNN, T., MURPHY, J.R., CHIZEK, M., RIDLEY, A. (2015). Mars Global Ionosphere-Thermosphere Model (MGITM): Solar cycle, seasonal, and diurnal variations of the Mars upper atmosphere. *J. Geophys. Res. Planets.* 120, 311–342. doi:10.1002/2014JE004715.
- CAIN, J. C., FERGUSON, B.B., MOZZONI, D. (2003). An $n = 90$ internal potential function of the Martian crustal magnetic field. *J. Geophys. Res.* 108(E2), 5008. doi:10.1029/2000JE001487.
- CARTACCI, M., AMATA, E., CICHETTI, A., NOSCHESI, R., GIUPPI, S., LANGLAIS, B., FRIGERI, A., OROSEI, R., PICARDI, G. (2013). Mars ionosphere total electron content analysis from MARSIS subsurface data. *Icarus.* 223, 1, 423–437. doi:10.1016/j.icarus.2012.12.011.
- CHICARRO, A., MARTIN, P., TRAUNTER, R. (2004). Mars Express: A European Mission to the Red Planet. *Eur. Space Agency Publ. Div., Noordwijk, Netherlands* SP-1240, pp. 3–16.
- GONZÁLEZ-GALINDO, F., CHAUFRAY, J.-Y., LÓPEZ-VALVERDE, M.A., GILLI, G., FORGET, F., LEBLANC, F., MODOLO, R., HESS, S., YAGI, M. (2013). Three-dimensional Martian ionosphere model: I. The photochemical ionosphere below 180 km. *J. Geophys. Res. Planets.* 118, 2105–2123. doi:10.1002/jgre.20150.
- GURNETT, D.A., KIRCHNER, D.L., HUFF, R.L., MORGAN, D.D., PERSON, A.M., AVERKAMP, T.F., DURU, F., NIELSEN, E., SAFAEINILI, A., PLAUT, J.J., PICARDI, G. (2005). Radar soundings of the ionosphere of Mars. *Science.* 310, 1999–1933. doi:10.1126/science.1121868.
- KLENZING, J., SIMOES, F., IVANOV, S., BILITZA, D., HEELIS, R.A., ROWLAND, D. (2013). Performance of the IRI-2007 model for equatorial topside ion density in the African sector for low and extremely low solar activity, *Adv. Space Res.* 52, 1780–1790. doi:10.1016/j.asr.2012.09.030.
- KUTIEV, I., et al. (2013). Solar activity impact on the Earth's upper atmosphere. *J. Space Weather Space Clim.* 3, A06.DOI: 10.1051/swsc/2013028
- MATTA, M., MENDILLO, M., WITHERS, P., MORGAN, D.D. (2015). Interpreting Mars ionospheric anomalies over crustal magnetic field regions using a 2-D iono-

- spheric model. *J. Geophys. Res. Space Physics.* 120, 766–777. doi:10.1002/2014JA020721.
- MENDILLO, M., WITHERS, P., HINSON, D., RISHBETH, H., REINISCH, B. (2006). Effects of solar flares on the ionosphere of Mars. *Science.* 311, 1135–1138. doi: 10.1126/science.1122099
- MOREL, L., WITASSE, O., WARNANT, R., CERISIER, J.-C., BLELLY, P.-L., LILENSTEN, J. (2004). Diagnostic of the dayside ionosphere of Mars using the Total Electron Content measurement by the NEIGE/Netlander experiment: An assessment study. *Planetary and Space Science.* 52, 7, 603–611. doi:10.1016/j.pss.2003.12.007.
- MORGAN, D. D., WITASSE, O., NIELSEN, E., GURNETT, D.A., DURU, F., KIRCHNER, D.L. (2013). The processing of electron density profiles from the Mars Express MARSIS topside sounder. *Radio Sci.* 48, 197–207. doi:10.1002/rds.20023.
- NĚMEC, F., MORGAN, D. D., GURNETT, D.A., DURU, F., TRUHLIK, V. (2011). Dayside ionosphere of Mars: Empirical model based on data from the MARSIS instrument. *J. Geophys. Res.* 116, E07003, doi:10.1029/2010JE003789.
- NĚMEC, F., MORGAN, D. D., GURNETT, D.A., ANDREWS, D.J. (2016). Empirical model of the Martian dayside ionosphere: Effects of crustal magnetic fields and solar ionizing flux at higher altitudes. *J. Geophys. Res. Space Physics.* 121, 1760–1771, doi:10.1002/2015JA022060.
- OROSEI, R., et al. (2014). Mars Advanced Radar for Subsurface and Ionospheric Sounding (MARSIS) after nine years of operation: A summary. *Planetary and Space Science.* <http://dx.doi.org/10.1016/j.pss.2014.07.010>
- PETER, K., et al. (2014). The dayside ionospheres of Mars and Venus: Comparing a one-dimensional photochemical model with MaRS (Mars Express) and VeRa (Venus Express) observations. *Icarus.* 233, 66–82. <http://dx.doi.org/10.1016/j.icarus.2014.01.028>
- PICARDI, G., et al. (2004). Mars Express: A European Mission to the Red Planet, MARSIS: Mars Advanced Radar for Subsurface and Ionosphere Sounding. *Eur. Space Agency Publ. Div., Noordwijk, Netherlands.* SP-1240, pp. 51–70.
- RAMSTAD, R., BARABASH, S., FUTAANA, Y., NILSSON, H., WANG, X.-D., HOLMSTRÖM, M. (2015). The Martian atmospheric ion escape rate dependence on solar wind and solar EUV conditions: 1. Seven years of Mars Express observations. *J. Geophys. Res. Planets.* 120, 1298–1309. doi:10.1002/2015JE004816.
- SÁNCHEZ-CANO, B., WITASSE, O., HERRAIZ, M., RADICELLA, S.M., BAUER, J., BLELLY, P.-L., RODRÍGUEZ-CADEROT, G. (2012). Retrieval of ionospheric profiles from the Mars Express MARSIS experiment data and comparison with radio-occultation data. *Geosci. Instrum. Method Data Syst.* 1, 77–84. doi:10.5194/gi-1-77-2012.
- SÁNCHEZ-CANO, B., RADICELLA, S. M., HERRAIZ, M., WITASSE, O., RODRÍGUEZ – CADEROT, G. (2013). NeMars: An empirical model of the Mar-

- tian dayside ionosphere based on Mars Express MARSIS data. *Icarus*. 225, 236-247. doi:10.1016/j.icarus.2013.03.021
- SÁNCHEZ-CANO, B. (2014). Ionosfera de Marte: calibración y análisis de datos, y modelado. Ionosphere of Mars: data calibration and analysis, and modelling. *PhD Thesis*. Universidad Complutense de Madrid. ISBN: 978-84-616-9995-7.
- SÁNCHEZ-CANO, B., et al. (2015a). Total Electron Content in the Martian atmosphere: a critical assessment of the Mars Express MARSIS datasets. *J. Geophys. Res. Space Physics*. 120, 2166–2182, doi:10.1002/2014JA020630.
- SÁNCHEZ – CANO, B., LESTER, M., WITASSE, O., MILAN, S.E., HALL, B.E.S., BLELLY, P.-L., RADICELLA, S. M., MORGAN, D.D. (2015b). Evidence of scale height variations in the Martian ionosphere over the solar cycle. *J. Geophys. Res. Space Physics*. 120, 10,913–10,925. doi:10.1002/2015JA021949.
- SÁNCHEZ-CANO, B., LESTER, M., WITASSE, O., MILAN, S.E., HALL, B.E.S., CARTACCI, M., PETER, K., MORGAN, D.D., BLELLY, P.-L., RADICELLA, S.M., CICCETTI, A., NOSCHESI, R., OROSEI, R., PÄTZOLD, M. (2016). Solar cycle variations in the ionosphere of Mars as seen by multiple Mars Express datasets. *J. Geophys. Res. Space Physics*. 120, doi: 10.1002/2015JA022281.
- SCHUNK, R., NAGY, A.F. (2009). Ionospheres: Physics, Plasma Physics, and Chemistry. *Cambridge University Press*. ISBN 978-0-521-87706-0.
- SHINAGAWA, H., CRAVENS, T.E. (1989). A one-dimensional multispecies magnetohydrodynamic model of the dayside ionosphere of Mars. *J. Geophys. Res.* 94, A6, 6506-6516.
- SOLOMON, S. C., WOODS, T. N., DIDKOVSKY, L. V., EMMERT, J. T., QIAN, L. (2010). Anomalously low solar extreme-ultraviolet irradiance and thermospheric density during solar minimum. *Geophys. Res. Lett.* 37, L16103 doi:10.1029/2010GL044468.
- SOLOMON, S. C., QIAN, L., DIDKOVSKY, L. V., VIERECK, R. A., WOODS, T. N. (2011). Causes of low thermospheric density during the 2007–2009 solar minimum. *J. Geophys. Res.* 116, A00H07. doi:10.1029/2011JA016508.
- SOLOMON, S. C., QIAN, L., BURNS, A. G. (2013). The anomalous ionosphere between solar cycle 23 and 24. *J. Geophys. Res. Space Physics*. 118,6524–6535. doi:10.1002/jgra.50561.
- WANG, J.-S., NIELSEN, E. (2004). Evidence for topographic effects on the Martian ionosphere. *Planetary and Space Science*. 52, 9, 881-886. doi:10.1016/j.pss.2004.01.008
- WITASSE, O. (2000). Modélisation des Ionosphères planétaires et de leur Rayonnement: la Terre et Mars. *PhD Thesis*. Laboratoire de Planétologie de Grenoble.
- WITASSE, O., CRAVENS, T., MENDILLO, M., MOSES, J., KLIORÉ, A., NAGY, F., BREUS, T. (2008). Solar System Ionospheres. *Space Sci Rev.* 139, 235–265. doi:10.1007/s11214-008-9395-3.

- WITHERS, P., BOUGHER, S.W., KEATING, G.M. (2003). The effects of topographically-controlled thermal tides in the Martian upper atmosphere as seen by the MGS accelerometer. *Icarus*. 164, 14–32, doi:10.1016/S0019-1035(03)00135-0
- WITHERS, P. (2009). A review of observed variability in the dayside ionosphere of Mars. *Advances in Space Research*. 44, 277-307. doi:10.1016/j.asr.2009.04.027
- WITHERS, P., FALLOWS, K., GIRAZIAN, Z., MATTA, M., HÄUSLER, B., HINSON, D., TYLER, L., MORGAN, D.D., PÄTZOLD, M., PETER, K., TELLMANN, S., PERALTA, J., WITASSE, O. (2012a). A clear view of the multifaceted dayside ionosphere of Mars. *Geophys. Res. Lett.* 39, L18202. doi:10.1029/2012GL053193.
- WITHERS, P., FILLINGIM, M.O., LILLIS, R.J., HÄUSLER, B., HINSON, D.P., TYLER, G.L., PÄTZOLD, M., PETER, K., TELLMANN, S., WITASSE, O. (2012b). Observations of the nightside ionosphere of Mars by the Mars Express Radio Science Experiment (MaRS). *J. Geophys. Res.* 117, A12307. doi:10.1029/2012JA018185.
- WITHERS, P., PRATT, R. (2013). An observational study of the response of the upper atmosphere of Mars to lower atmospheric dust storms. *Icarus*. 225, 378–389. <http://dx.doi.org/10.1016/j.icarus.2013.02.032>
- WITHERS, P., MORGAN, D. D., GURNETT, D. A. (2014). Variations in peak electron densities in the ionosphere of Mars over a full solar cycle. *Icarus*. 251, 5–11. doi:10.1016/j.icarus.2014.08.008.
- WOODS, T. N., EPAVIER, F. G. (2006). Solar ultraviolet variability during the TIMED mission. *Adv. Space Res.* 37, 219–224. doi:10.1016/j.asr.2004.10.006.
- YUE, X., SCHREINER, W.S., ROCKEN, C., KUO, Y.-H. (2013). Validate the IRI2007 model by the COSMIC slant TEC data during the extremely solar minimum of 2008. *Adv. Space Res.* 51, 647–653. doi:10.1016/j.asr.2011.08.011.
- ZOU, H., LILLIS, R.J., WANG, J.S., NIELSEN, E. (2011). Determination of seasonal Variations in the Martian Neutral Atmosphere from Observations of Ionospheric Peak Height. *J. Geophys. Res.* 116. E09004, doi:201110.1029/2011JE003833.